



# Preparation of Pt–Ru catalysts on Nafion(Na<sup>+</sup>)-bonded carbon layer using galvanostatic pulse electrodeposition for proton-exchange membrane fuel cell

Youngmi Ra<sup>a</sup>, Jaeseung Lee<sup>b</sup>, In Kim<sup>a</sup>, Sungyool Bong<sup>a</sup>, Hasuck Kim<sup>a,\*</sup>

<sup>a</sup> Department of Chemistry, Seoul National University, San 56-1, Sillim 9-dong, Kwanak-gu, Seoul 151-747, Republic of Korea

<sup>b</sup> Hyundai Motor Company, 104 Mabuk-dong, Giheung-gu, Yongin-si, Gyeonggi-do 446-912, Republic of Korea

## ARTICLE INFO

### Article history:

Received 30 May 2008

Received in revised form 15 August 2008

Accepted 26 October 2008

Available online 21 November 2008

### Keywords:

Proton-exchange membrane fuel cell

Electrodeposition

Platinum–ruthenium alloy

Catalyst utilization efficiency

Carbon dioxide tolerance

## ABSTRACT

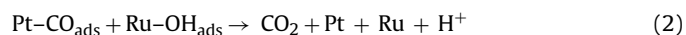
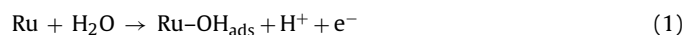
Platinum–ruthenium (Pt–Ru) on a Nafion(Na<sup>+</sup>)-bonded carbon layer is fabricated by using galvanostatic pulse electrodeposition for high utilization of catalysts and cost reduction. The composition of the Pt–Ru electrode, which is controlled by varying the concentration of the Ru precursor, is determined by inductively coupled plasma-atomic emission spectroscopy and by electron probe microanalysis. The particle size of the electrodeposited Pt–Ru catalyst is determined by high-resolution transmission electron microscopy. Other characterizations are carried out by X-ray diffraction, X-ray photoelectron spectroscopy, and CO-stripping voltammetry. Electrodeposited Pt–Ru catalysts give improved performance, not only in single-cell operations but also with respect to CO tolerance compared with electrodes prepared by conventional means. The behaviour is probably due to enhanced utilization of the catalysts. Recovery from CO exposure demonstrates that the electrodeposited catalysts exhibit better resistance to CO.

© 2008 Elsevier B.V. All rights reserved.

## 1. Introduction

Among the various fuel cells, proton-exchange membrane fuel cells (PEMFCs) as energy conversion devices are promising future power systems with high power density, energy efficiency, and low operating temperature [1–4]. Nevertheless, a PEMFC operating with hydrogen (H<sub>2</sub>) gas containing carbon monoxide (CO) from the reforming of fossil fuels shows low performance. This problem is caused by CO poisoning of the catalyst. The gas blocks the Pt surface because the bond strength of Pt–CO is greater than that of Pt–H, and thereby decreases the activity of the anode [5–8].

In order to improve the CO tolerance of the anode, many studies in recent years have reported details of new preparation methods and different compositions of Pt-based catalysts such as Pt–Ru, Pt–Sn and Pt–Mo [5,6,8–12]. In particular, the Pt–Ru system is an excellent anode electrocatalyst since it exhibits enhanced CO tolerance, which can be attributed to a bifunctional mechanism as follows [12]:



Pt–Ru electrodes for PEMFCs [13] have been prepared by various methods such as the colloidal [14,15], impregnation [16] and

electrodeposition [5,17–19] methods. Catalyst powders synthesized by means of the colloidal and impregnation methods were well-mixed with ionic binder (e.g., Nafion solution) and then spread on a gas diffusion layer (GDL). After this procedure, the membrane electrode assembly (MEA) was generally fabricated using the prepared electrode and a Nafion membrane. This method does, however, produce a large number of inactive catalyst sites because the catalytic reaction occurs only at the interface between the membrane and the electrode that is exposure to the reactant, known as the triple-phase boundary (Fig. 1(a)) [17]. Also, ionic binder is added to the electrode in order to extend the triple-phase boundaries. As the result, it increases the production cost of the electrode [20].

The electrodeposition method – a way to overcome the cost problem – makes catalysts that are deposited directly on the surface of the substrate. Therefore, it offers not only enhanced catalyst utilization (Fig. 1(b)) but also simplification of preparation. In general, electrodeposition can be carried out by using either a potentiostatic [23–25] or galvanostatic method, which involves direct and pulse techniques. Electrodeposition via the galvanostatic pulse technique is considered convenient to improve the current distribution, therefore, it is easy to control the particle size and composition of the alloy simply by varying experimental parameters such as on/off time and peak current density [20–22]. Coutanceau et al. [18] and Wei and Chan [19] reported the preparation of an Pt–Ru anode for direct methanol fuel cells by using a galvanostatic pulse technique. They obtained catalysts with a 1:1 atomic ratio and improved performance. Alcaide et al. [5] obtained enhanced CO

\* Corresponding author. Tel.: +82 2 880 6638; fax: +82 2 880 6638.

E-mail address: [hasuckim@snu.ac.kr](mailto:hasuckim@snu.ac.kr) (H. Kim).

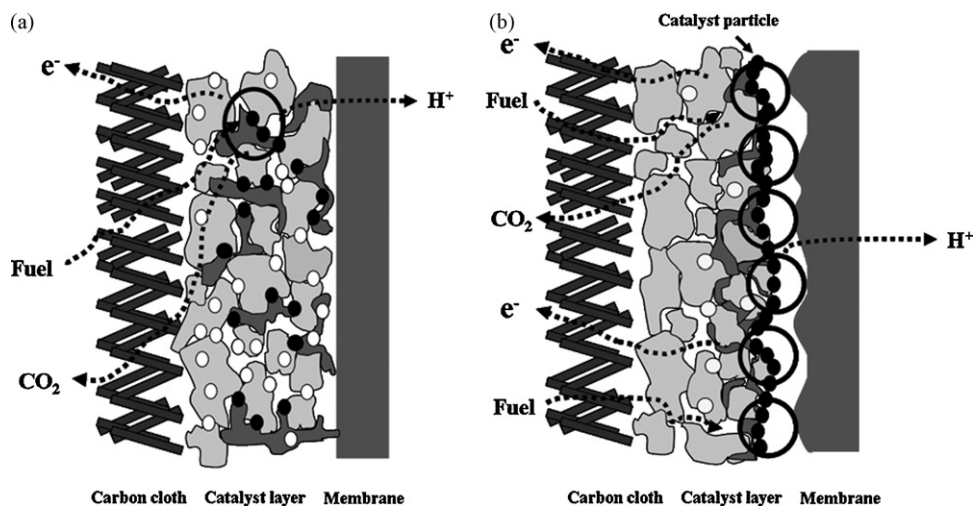


Fig. 1. Schematic diagrams of anode prepared by (a) colloidal or impregnation method and (b) electrodeposition and transport of fuel, protons and electrons.

tolerance from an electrodeposited Pt–Ru anode for in a H<sub>2</sub>-fed PEMFC.

The aim of this investigation is to characterize electrochemically deposited Pt–Ru catalysts prepared by various physical and electrochemical methods, and to achieve improved performance

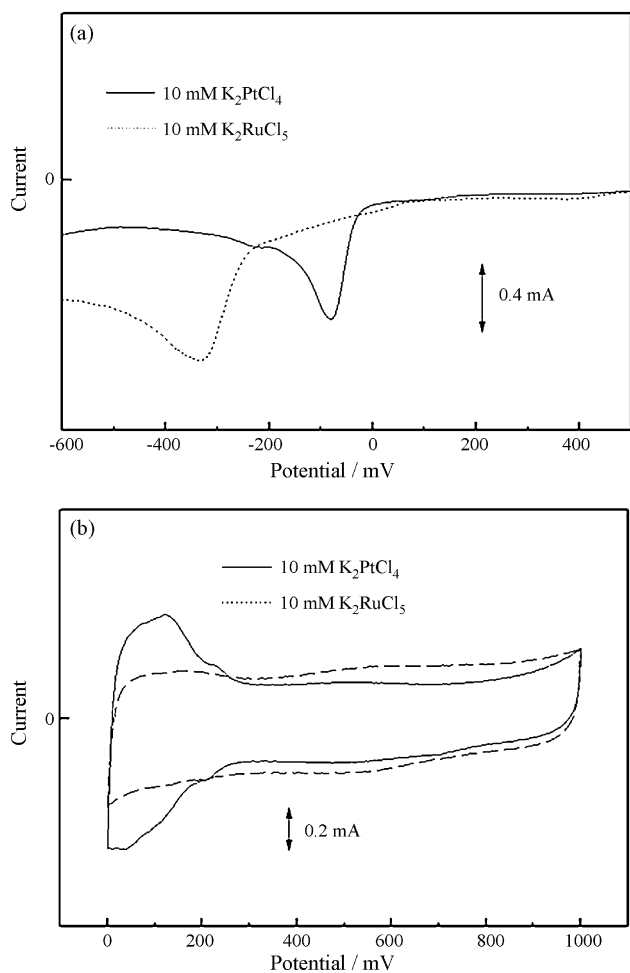


Fig. 2. Deposition behaviour of Pt and Ru on Nafion(Na<sup>+</sup>)-bonded carbon layer: (a) potential sweep electroreduction on Nafion(Na<sup>+</sup>)-bonded carbon layer; (b) cyclic voltammograms of deposited Pt and Ru in 1 M H<sub>2</sub>SO<sub>4</sub> solution at scan rate of 20 mV s<sup>-1</sup>.

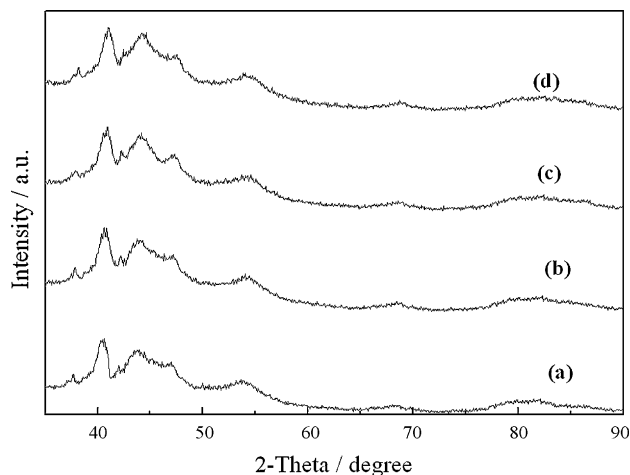


Fig. 3. XRD patterns of Pt–Ru catalysts deposited from 20 mM K<sub>2</sub>PtCl<sub>4</sub> and various concentrations of K<sub>2</sub>RuCl<sub>5</sub>: (a) 10, (b) 20, (c) 30 and (d) 40 mM.

in terms of overall cell operation and CO tolerance compared with commercial Pt–Ru catalysts.

## 2. Experimental

### 2.1. Deposition of Pt and Ru on Nafion(Na<sup>+</sup>)-bonded carbon electrode: potential sweep method

Prior to the electrodeposition of Pt–Ru catalysts, the deposition behaviour of Pt and Ru on Nafion(Na<sup>+</sup>)-bonded carbon electrode was studied with an electrochemical analyzer (BAS, 100B/W, Bioanalytical Systems). With a three-electrode cell system, each Nafion(Na<sup>+</sup>)-bonded carbon electrode was used as a working

Table 1

Amount of Pt and Ru (mg cm<sup>-2</sup>) of deposits from 20 mM Pt and various concentrations of K<sub>2</sub>RuCl<sub>5</sub>.

Samples	Pt	Ru
10 mM K <sub>2</sub> RuCl <sub>5</sub>	0.0630	0.0115
20 mM K <sub>2</sub> RuCl <sub>5</sub>	0.0651	0.0225
30 mM K <sub>2</sub> RuCl <sub>5</sub>	0.0770	0.0415
40 mM K <sub>2</sub> RuCl <sub>5</sub>	0.0779	0.0557

Measured by ICP-AES.

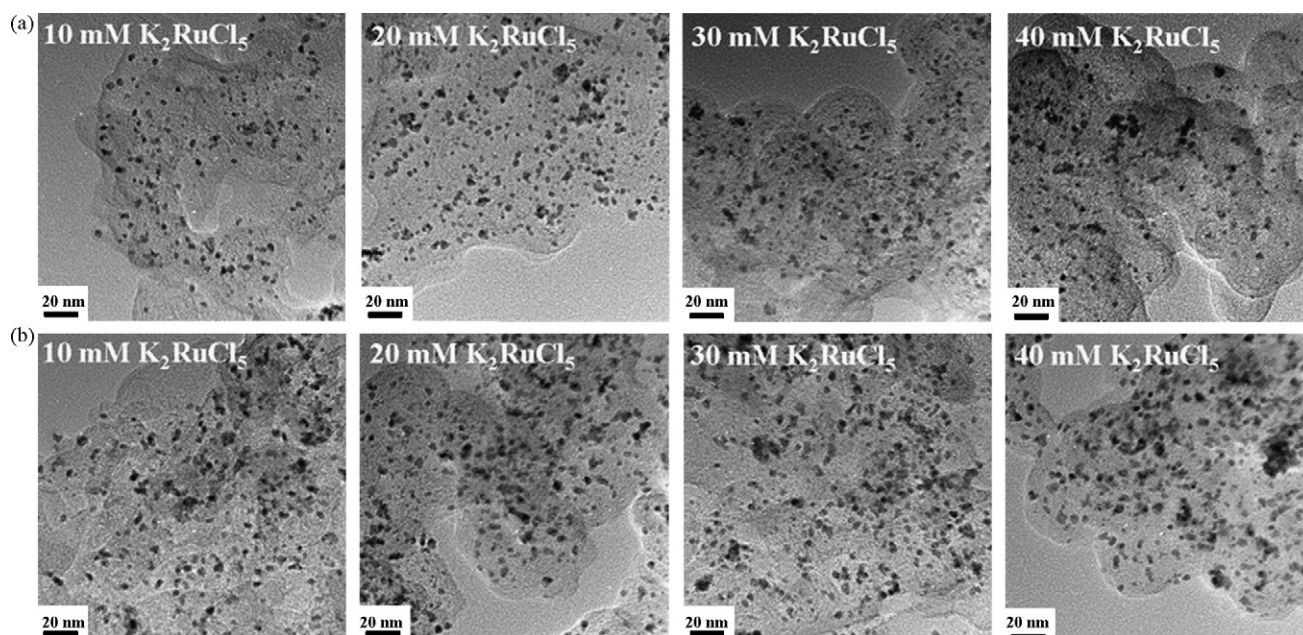


Fig. 4. High-resolution transmission electron micrographs (HR-TEM) of electrodeposited PtRu catalysts: (a) before heat treatment; (b) after heat treatment.

**Table 2**  
EPMA and ICP-AES results of chemical composition for prepared catalysts.

Samples	Pt:Ru atomic ratio	
	ICP-AES measurement	EPMA measurement
10 mM $K_2RuCl_5$	74:26	75:25
20 mM $K_2RuCl_5$	60:40	59:41
30 mM $K_2RuCl_5$	49:51	49:51
40 mM $K_2RuCl_5$	42:58	44:56

electrode while a Pt foil served as the counter electrode and an Ag|AgCl electrode as the reference electrode. Nafion( $Na^+$ )-bonded carbon electrodes were prepared on glassy carbon electrodes by spraying with carbon slurry. The carbon slurry was made by mixing 0.1 g Vulcan XC-72 carbon powder, 0.43 ml Nafion solution (Aldrich, 5 wt.% 1100 EW) with 6 ml isopropyl alcohol in an ultrasonic bath. Then, glycerol and excess sodium hydroxide were added to the mixture to form a hydrophilic layer and to convert the  $H^+$ -form of Nafion to the  $Na^+$ -form. These steps which increase the current efficiency and thermal stability, respectively.

In order to use the  $Na^+$ -form of Nafion, it is also necessary to render precursors and electrolytes free of protons [17]. Therefore, 10 mM  $K_2PtCl_4$ , 10 mM  $K_2RuCl_5$ , and 0.5 M NaCl were used as the Pt precursor, Ru precursor and electrolyte, respectively. Also 0.4 M ethyl alcohol was added to the solution to avoid the formation of undesirable products on the counter electrode.

Pt and Ru were first electrodeposited on Nafion( $Na^+$ )-bonded carbon electrodes by using the potential sweep method. The potential was scanned from 500 to  $-600$  mV (vs. standard hydrogen electrode (SHE)) at a scan rate of  $10$  mV  $s^{-1}$ . After Pt and Ru deposition, the electrode was rinsed with ultrapure water and then the electrochemical properties were assessed in 1 M  $H_2SO_4$  solution by cyclic voltammetry. Cyclic voltammograms (CVs) were generally recorded at a scan rate of  $20$  mV  $s^{-1}$ . All potentials are reported with respect to the SHE.

## 2.2. Preparation of Nafion( $Na^+$ )-bonded carbon electrodes

To apply a uniform electrode surface, a gas-diffusion layer (GDL; E-TEK, LT 1200-W) was used as a backing layer. The car-

bon slurry was applied to the hydrophobic GDL by spraying to form a hydrophilic layer. The hydrophilic layer was loaded with  $0.3$  mg  $cm^{-2}$  of carbon.

## 2.3. Electrodeposition

Galvanostatic pulse electrodeposition of Pt–Ru electrodes was performed using a two-electrode cell and an electrochemical system (VoltaLab80, Radiometer). The Nafion( $Na^+$ )-bonded carbon electrode served as the cathode and Pt mesh as the anode. The electrodes were mounted on a sample holder coupled to Pt foil as a current-collector. The plating bath was a solution composed of 20 mM  $K_2PtCl_4$  and various concentrations of  $K_2RuCl_5$  (10, 20, 30, and 40 mM) dissolved in 0.5 M NaCl and 0.4 M ethyl alcohol. The sample holder was immersed in the plating bath for 5 min so that the carbon electrode was soaked sufficiently. The parameters for galvanostatic pulse electrodeposition were a peak current density of  $300$  mA  $cm^{-2}$ , an on/off time of 10/100 ms and a total charge density of  $1$  C  $cm^{-2}$ .

After electrodeposition, the electrode was rinsed with ultrapure water to remove any residue of precursors and chloride ions that degrade the cell performance [26].

## 2.4. Characterization of electrodeposited Pt–Ru catalysts

The chemical composition of the Pt–Ru catalysts were obtained by using an electron probe micro-analyzer (EPMA, JEOL Co., JXA-8900R) and the amount of metals in the electrodeposited catalysts was determined by inductively coupled plasma-atomic emission spectroscopy (ICP-AES). The morphology and particle size of the electrodeposited Pt–Ru catalysts were obtained with a high-resolution transmission electron microscope (HR-TEM, JEOL Co., JEM-200CX). After electrodeposition, the catalysts were heat-treated at  $250$  °C in  $H_2$  (10%)/ $N_2$  (90%) gas for 30 min to remove organic solvent and reduce the oxidized catalysts. Before and after the heat treatment, the oxidation states of Pt were analyzed by X-ray photoelectron spectroscopy (XPS, Pohang Accelerator Laboratory, Beam line 4B1). Data from X-ray diffraction measurements (XRD, Philips, X'pert APD) were analyzed for the degree of alloying and lattice parameters.

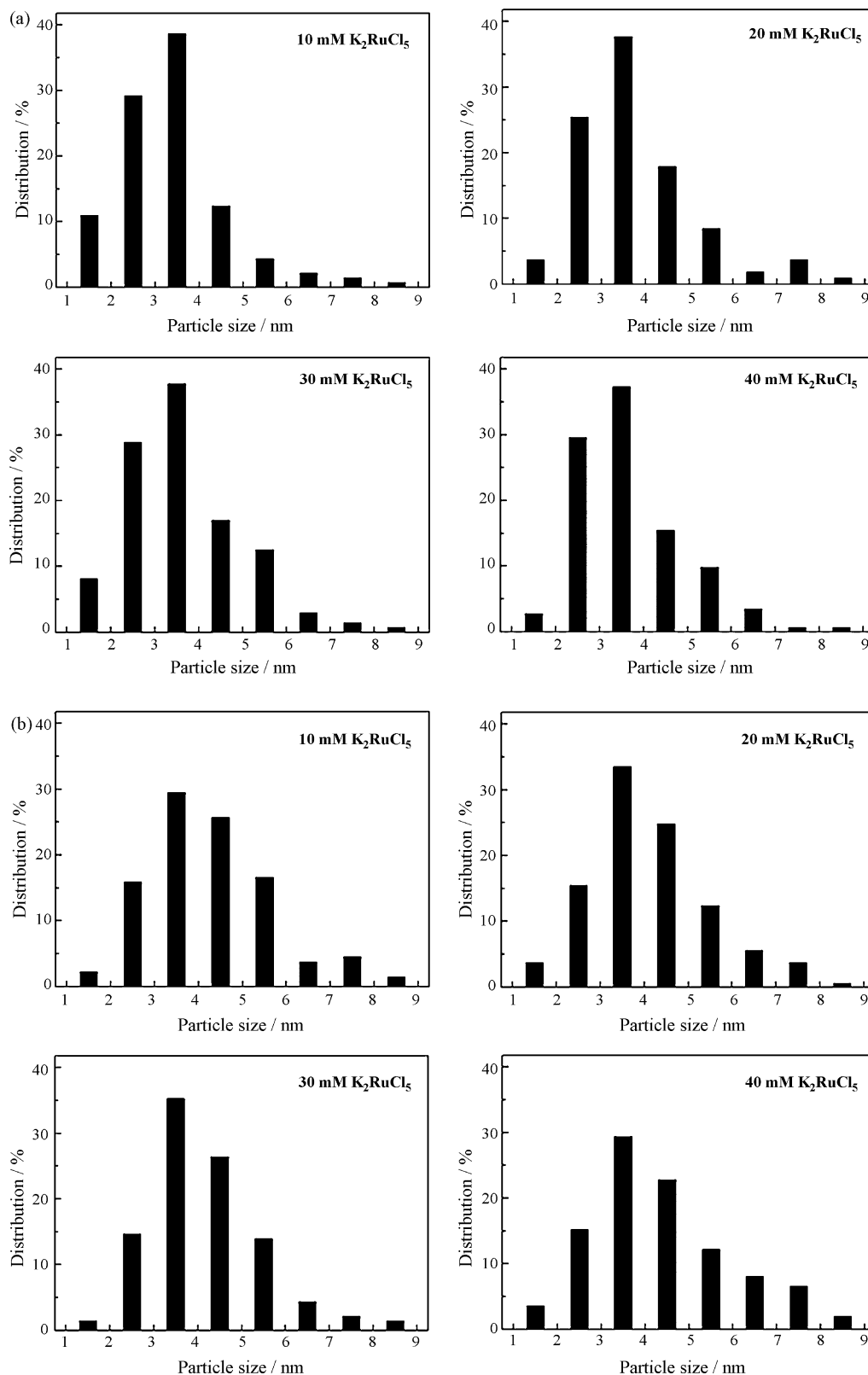


Fig. 5. Particle-size distribution of prepared catalysts by HR-TEM: (a) before heat treatment; (b) after heat treatment.

For CO-stripping voltammetry, CO was adsorbed at a potential of 100 mV (vs. SHE) in CO-saturated 1 M  $H_2SO_4$  solution for 10 min, and then the electrolyte was purged with  $N_2$  for 10 min to remove dissolved CO. The voltammograms were recorded from 0 to 800 mV at  $20\text{ mV s}^{-1}$ .

### 2.5. MEA fabrication and single-cell operation

A commercial 40 wt.% Pt/C from E-TEK and 5 wt.% Nafion solution were thoroughly mixed with isopropyl alcohol to make the cathodes. The well-mixed slurry was sprayed on a GDL (E-TEK, LT

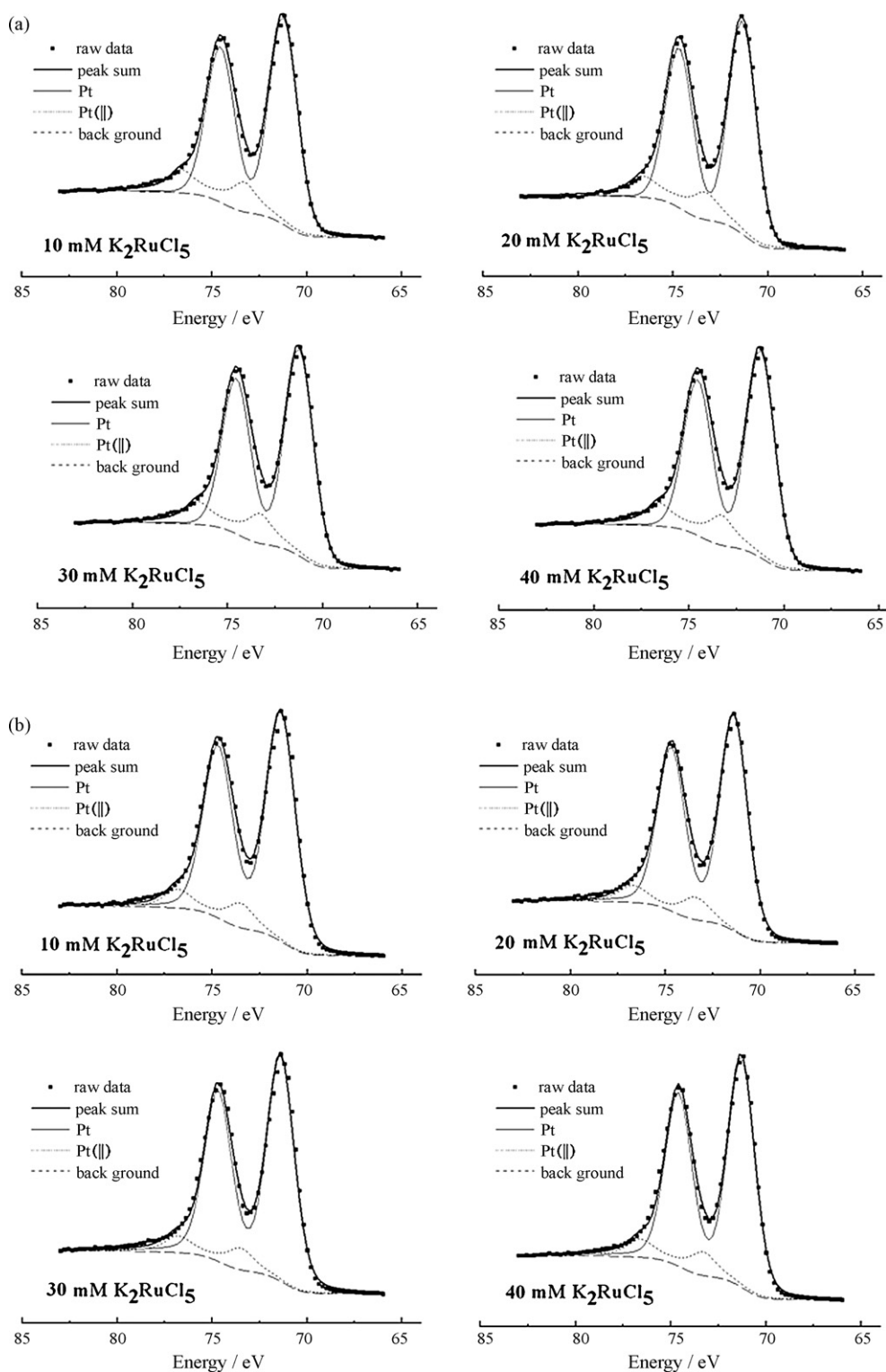


Fig. 6. X-ray photoelectron spectra of Pt 4f of prepared catalysts: (a) before heat treatment; (b) after heat treatment.

1200-W) at  $0.4 \text{ mg cm}^{-2}$ . The electrodeposited Pt–Ru electrode, the splayed Pt electrode and a Nafion membrane (DuPont) were used to form a membrane-electrode assembly (MEA) by hot pressing at  $130^\circ\text{C}$  for 3 min at  $100 \text{ kgf cm}^{-2}$ . For comparison, a conventional MEA was also fabricated by using 40 wt.% Pt/Ru/C (E-TEK,  $0.118 \text{ mg}_{\text{PtRu}} \text{ cm}^{-2}$ ) and 40 wt.% Pt/C (E-TEK,  $0.4 \text{ mg cm}^{-2}$ ) as the anode and the cathode, respectively.

The operating conditions (temperature, gas flow rate) for single-cell performance tests were controlled by a test station (Globe Tech, Inc. 890 series, GT-500). The cell temperature was maintained at  $70^\circ\text{C}$  with  $\text{H}_2$  and air gas humidified at 75 and  $80^\circ\text{C}$ , respectively. The pressures on both electrodes were maintained at 2 bar.

After obtaining the single-cell performances of the electrodeposited and commercial electrodes, the CO tolerance, of each



electrode was evaluated by exposure to H<sub>2</sub>/CO (10 ppm) gas for 1 h, and then pure H<sub>2</sub> gas for 1 h.

### 3. Results and discussion

#### 3.1. Deposition of Pt and Ru on Nafion(Na<sup>+</sup>)-bonded carbon layers

Pt and Ru were electrodeposited on a Nafion(Na<sup>+</sup>)-bonded carbon layer to investigate the deposition pattern of precursors, because this depends on the type of ligands, electrolytes, additives and deposition conditions [17]. Fig. 2(a) shows the deposition behaviour from K<sub>2</sub>PtCl<sub>4</sub> and K<sub>2</sub>RuCl<sub>5</sub> on a carbon layer, and Fig. 2(b) presents the electrochemical properties of deposited electrodes in 1 M H<sub>2</sub>SO<sub>4</sub>. According to Fig. 2(a), the beginning of Ru deposition appears easier than that of Pt but the reduction peak ( $E_p = -334$  mV) of Ru is observed at a more negative potential than that ( $E_p = -81$  mV) of Pt. Therefore, the overpotential for Ru nucleation on carbon surface is larger than that of Pt. After deposition, CVs were recorded from 0 to 1000 mV vs. SHE at 20 mV s<sup>-1</sup> in H<sub>2</sub>SO<sub>4</sub> (Fig. 2(b)). This results show that the adsorption/desorption hydrogen peak for deposited Ru is almost absent compared with Pt but it has a thicker double-layer region.

#### 3.2. Galvanostatic pulse electrodeposition from K<sub>2</sub>PtCl<sub>4</sub> and K<sub>2</sub>RuCl<sub>5</sub> on Nafion(Na<sup>+</sup>)-bonded carbon electrodes

Electrodes made by the electrodeposition method have several advantages such as enhanced catalyst utilization, cost reduction, and simplification of preparation. Based on these advantages, many workers have been reported the performance and characteristics of electrodeposited electrodes [11,22,23,27].

Under our optimized conditions, Pt–Ru catalysts were prepared on Nafion(Na<sup>+</sup>)-bonded carbon layers by means of a galvanostatic method. The electrodes, prepared by varying K<sub>2</sub>RuCl<sub>5</sub> concentrations with a peak current density of 300 mA cm<sup>-2</sup>, a on/off time of 10/100 ms and a total charge density of 1 C cm<sup>-2</sup>, were characterized by XRD, EPMA, ICP-AES, TEM, and XPS.

X-ray diffraction patterns were analyzed to investigate the structural change when platinum is alloyed with ruthenium. The XRD patterns of the electrodeposited Pt–Ru catalysts are presented in Fig. 3. The platinum (1 1 1) peak of Pt–Ru electrodes shifts to a higher angle compared with the pure platinum peak from JCPDS (#4-0802) to indicate that there is alloy formation between platinum and ruthenium. The lattice parameters were evaluated from (1 1 1), (2 0 0), (2 2 0), and (3 1 1) peaks. These values are 3.899, 3.893, 3.883 and 3.885 Å for Fig. 3(a)–(d), respectively, but the average particle size could not be calculated because of a weak (2 2 0) peak in the XRD patterns. This phenomenon can be explained by the relatively low loading of the catalysts. Therefore, the particle size of electrodeposited Pt–Ru catalysts was obtained by high-resolution transmission electron microscopy (HR-TEM).

The amount of loaded Pt and Ru was controlled by varying the concentration of K<sub>2</sub>RuCl<sub>5</sub> and then determined by ICP-AES, as shown in Table 1. The concentration of Ru precursor was varied from 10 to 40 mM while the concentration of Pt precursor was fixed at 20 mM. The data in Table 1 show that the amounts of Pt and Ru increase as the concentration of Ru precursor is increased, and these values are used to calculate the chemical composition and electrochemical surface area of electrodeposited Pt–Ru catalysts.

The chemical composition of the Pt–Ru catalysts was also measured by EPMA, in which the average value was obtained from several different points. The compositions of catalysts measured by ICP-AES and EPMA are listed in Table 2. From these results, a reliable chemical composition of each of the electrodes from two analytical methods is obtained and the optimum atomic ratio of 1:1 Pt–Ru can be prepared from 20 mM Pt and 30 mM Ru precursors [28].

The HR-TEM images of electrodeposited Pt–Ru catalysts before and after heat treatment are shown in Fig. 4. The average particle size is calculated from the particle distributions presented in Fig. 5. Before heat treatment, the particle size of the alloyed particles is 3–4 nm, regardless of the concentration of K<sub>2</sub>RuCl<sub>5</sub> (Fig. 5(a)), but the average particle size of the Pt–Ru electrode heat-treated at 250 °C in H<sub>2</sub> (10%)/N<sub>2</sub> (90%) gas for 30 min grew a little (Fig. 5(b)). The increase in the particle size of catalyst after heat treatment has been already confirmed in our earlier work [17].

The X-ray photoelectron spectra of Pt 4f from the prepared catalysts before and after the heat treatment are displayed in Fig. 6. XPS measurements are used to define the oxidation state of electrodeposited Pt. The spectra can be deconvoluted into two components, labelled as Pt and Pt(II) with binding energies of 71.0 and 73.1 or 73.2, as shown in Table 3. The relative intensities (%) of metallic Pt and Pt(II) in deposited samples from different K<sub>2</sub>RuCl<sub>5</sub> concentrations are almost the same, and these values increase in general after heat treatment, as shown in Table 3. It is reasonable to assume that reduction of oxidized Pt occurs during the heat treatment. Analysis for ruthenium 3p and 3d is difficult, however, since the two peaks are weak and overlap with a huge carbon 1s peak.

In order to measure the electrochemical surface area (ESA), CO-stripping voltammetry was performed with Nafion(Na<sup>+</sup>)-bonded carbon layers that were sprayed on glassy carbon electrodes for comparison. The catalyzed electrode was made by using the conventional method for PEM electrodes. Then, CO was first adsorbed on Pt–Ru catalysts on Nafion(Na<sup>+</sup>)-bonded carbon layers and CO-stripping voltammograms were recorded from 0 to 800 mV at 20 mV s<sup>-1</sup>. The onset potentials for CO oxidation of Pt–Ru catalysts obtained by electrodeposition from 20 mM K<sub>2</sub>PtCl<sub>4</sub> and different concentrations of K<sub>2</sub>RuCl<sub>5</sub> at 10, 20, 30 and 40 mM are 0.49, 0.53, 0.49, and 0.50 mV, respectively, see Fig. 7. The peak potentials for these samples are observed at 0.69, 0.60, 0.59 and 0.61 mV, respectively. The amount of metals determined by ICP-AES is shown in Table 1 and 420 μC cm<sup>-2</sup> was used to calculate the ESA values. For Pt–Ru catalysts deposited from 20 mM K<sub>2</sub>PtCl<sub>4</sub> and concentrations

**Table 3**  
Binding energies and relative intensities of electrodeposited catalysts obtained by XPS measurements.

Samples	Species	Binding energies of 4f <sub>7/2</sub> (eV)	Relative intensities (%)	
			Before heat treatment	After heat treatment
10 mM K <sub>2</sub> RuCl <sub>5</sub>	Pt	71.0	84	90
	Pt(II)	73.1	16	10
20 mM K <sub>2</sub> RuCl <sub>5</sub>	Pt	71.0	83	90
	Pt(II)	73.2	17	10
30 mM K <sub>2</sub> RuCl <sub>5</sub>	Pt	71.0	84	90
	Pt(II)	73.1	16	10
40 mM K <sub>2</sub> RuCl <sub>5</sub>	Pt	71.0	83	90
	Pt(II)	73.2	17	10

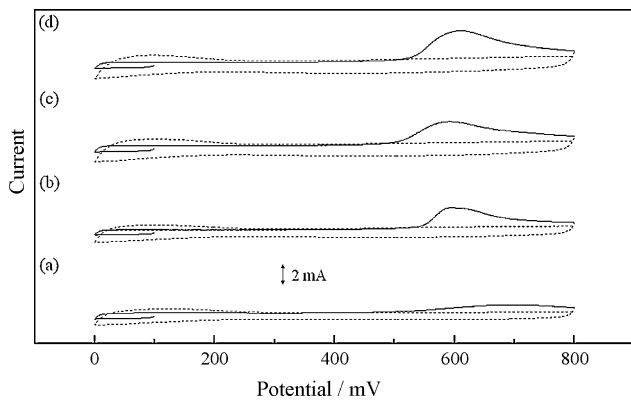


Fig. 7. CO-stripping voltammograms of deposits from 20 mM  $K_2PtCl_4$  and various concentrations of  $K_2RuCl_5$ : (a) 10, (b) 20, (c) 30 and (d) 40 mM.

of  $K_2RuCl_5$  of 10, 20, 30 and 40 mM, the ESA is 42.7, 107.4, 131.7, and  $115.7 \text{ m}^2 \text{ g}^{-1}$ , respectively. Thus, the electrode with a 1:1 PtRu atomic ratio made from 20 mM Pt and 30 mM Ru precursors has the highest ESA. These results show that Pt–Ru electrodes with different alloying states exhibit different abilities for CO oxidation and thereby affect the ESA of the prepared electrodes, though electrodes have similar particle sizes, as shown in Figs. 4 and 5. It is confirmed that electrodes of 1:1 PtRu atomic ratio exhibit excellent ability for CO oxidation and therefore they are evaluated for fuel cell performance and CO tolerance and compared with conventionally prepared electrodes.

3.3. Single-cell performance and CO tolerance

Fig. 8 presents the polarization curves of PEMFCs for anodes prepared by two different methods, namely, the electrodeposition and conventional methods. The electrodeposition method used 20 mM  $K_2PtCl_4$  and 30 mM  $K_2RuCl_5$  solutions. The amount of total metals in the electrode was determined as  $0.118 \text{ mg}_{PtRu} \text{ cm}^{-2}$  (Table 1).

Electrodes by the conventional method were prepared by spraying E-TEK catalysts on GDL. The cathode was made from a slurry of commercial 40 wt.% Pt/C E-TEK, Nafion solution and isopropyl alcohol. The mixture was sprayed on GDL with  $0.4 \text{ mg cm}^{-2}$  of Pt. When the same amount of Pt–Ru catalysts for both electrodeposited and conventional electrodes are used, the electrodeposited electrode

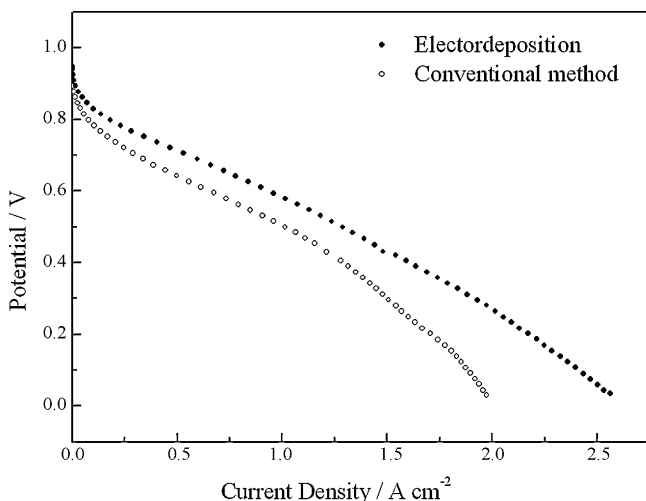


Fig. 8. Polarization curves of electrodeposited catalysts and 40 wt.% PtRu/C from E-TEK (conventional method). Operation conditions;  $T_{cell}$ :  $70^\circ\text{C}$ , 2 bar.

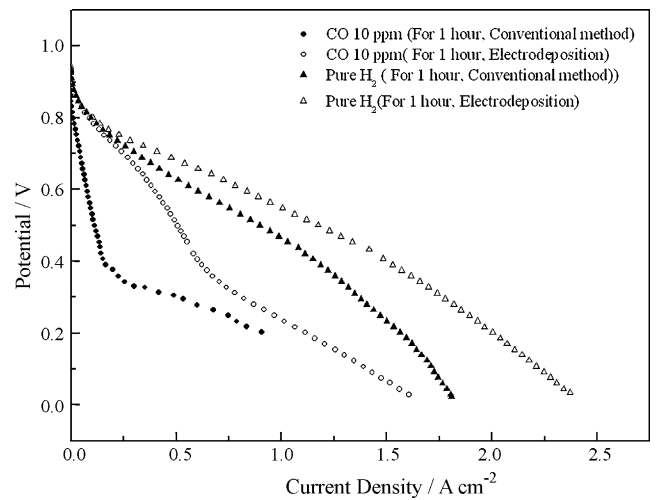


Fig. 9. Results after exposure to 10 ppm CO gas of electrodeposited and conventional electrodes.

exhibits better performance than the conventional electrode over the entire current density regions.

The polarization curves for  $H_2/CO$  (10 ppm) and recovery curves with electrodeposited and conventional electrodes are presented in Fig. 9. These results were obtained in following order: (i) after polarization curves of pure  $H_2$ , both electrodes were exposed to  $H_2/CO$  (10 ppm) for 1 h; (ii) conduct the performance test of electrodes; (iii) both electrodes were exposed to pure  $H_2$  for 1 h; (iv) obtain respective recovery curves. Performance of both electrodes that were exposed to CO gas for 1 h decreases but the electrodeposited Pt–Ru electrode shows better performance than the conventional electrode from E-TEK. Second, recovery curves do not reversibly return to the original performances even though the electrochemically deposited electrodes behaves better, as shown in Fig. 10.

The above findings indicate that the electrodeposited Pt–Ru catalyst on the Nafion( $Na^+$ )-bonded carbon layer is utilized more effectively due to the existence of abundant triple-phase boundaries, and also shows better CO tolerance than the conventional electrode from E-TEK with less metal loadings. Nevertheless, the original performance of the electrodes cannot be regained after exposure to CO gas. Nevertheless, the electrodeposited electrodes give closer-to-original recoveries against CO exposure.

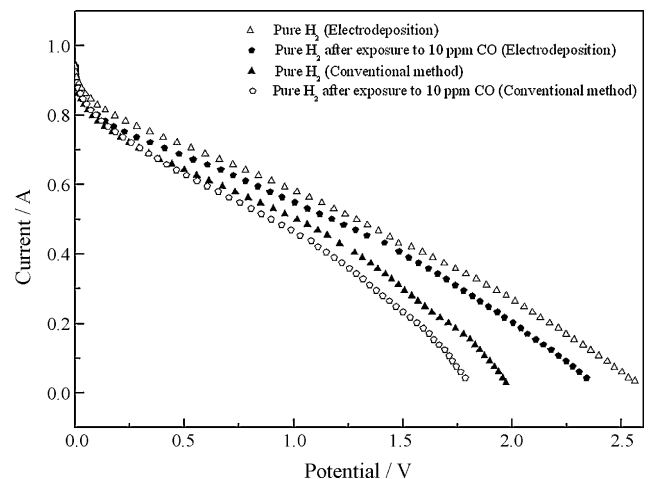


Fig. 10. Polarization curves before and after exposure to 10 ppm CO gas of electrodeposited and conventional electrodes.

#### 4. Conclusions

The characteristics and unit cell performance of Pt–Ru catalysts, prepared on Nafion(Na<sup>+</sup>)-bonded carbon electrode by galvanostatic pulse electrodeposition have been evaluated. The chemical composition of the electrodes is controlled by varying the concentration of Ru precursor. The average size of the Pt–Ru alloy particles is 3–4 nm, regardless of the concentration of K<sub>2</sub>RuCl<sub>5</sub>, and increases after heat treatment. From XPS studies, the oxidation state of Pt in all samples shows the same trend. Catalysts deposited from 20 mM Pt and 30 mM Ru precursors have an Pt:Ru atomic ratio of 1:1 and exhibit the largest electrochemical surface area (ESA) as obtained by CO-stripping voltammetry.

Electrodeposited Pt–Ru gives superior performance in single-cell operation, as well as greater CO tolerance compared with the electrodes prepared conventionally. This is probably due to enhanced utilization of catalysts. Recovery from CO exposure proves that electrodeposited catalysts exhibit better behaviour against the CO.

#### Acknowledgments

This work was supported by the Korea Science and Engineering Foundation (KOSEF) grant funded by the Korea Government (MEST) (No. R11-2005-008-00000-0) and BK 21 fellowship to Y. Ra and S. Bong.

#### References

- [1] J.H. Wee, K.Y. Lee, S.H. Kim, *J. Power Sources* 165 (2007) 667–677.
- [2] D. Hart, *J. Power Sources* 86 (2000) 23–27.
- [3] K.V. Kordesch, G.R. Simader, *Chem. Rev.* 95 (1995) 191–207.
- [4] M. Winter, R.J. Brodd, *Chem. Rev.* 104 (2004) 4245–4269.
- [5] F. Alcaide, O. Miguel, H.J. Grande, *Catal. Today* 116 (2006) 408–414.
- [6] D.C. Papageorgopolos, M.P. de Heer, M. Keijzer, J.A.Z. Pieterse, F.A. de Bruijin, *J. Electrochem. Soc.* 151 (2004) A763–A768.
- [7] E.I. Santiago, G.A. Camara, E.A. Ticianelli, *Electrochim. Acta* 48 (2003) 3527–3534.
- [8] J.B. Benziger, in: E. Shustorovich (Ed.), *Reaction Energies on Metal Surfaces: Theory and Applications*, ECH, New York, 1992, p. 53.
- [9] E.M. Crabb, R. Marshall, T. David, *J. Electrochem. Soc.* 147 (2000) 4440–4447.
- [10] T.J. Schmidt, Z. Jusys, H.A. Gasteiger, R.J. Behm, U. Endruschat, H. Boennemann, *J. Electroanal. Chem.* 501 (2001) 132–140.
- [11] R.C. Urian, A.F. Gulla, S. Mukerjee, *J. Electroanal. Chem.* 554–555 (2003) 307–324.
- [12] M. Watanabe, S. Motoo, *J. Electroanal. Chem.* 60 (1975) 275–283.
- [13] S. Litster, G. McLean, *J. Power Sources* 130 (2004) 61–76.
- [14] M. Watanabe, M. Uchida, S. Motoo, *J. Electroanal. Chem.* 229 (1987) 395–406.
- [15] H. Bonnemant, W. Brijoux, R. Brimkmann, E. Dinjus, T. Jousset, B. Korall, *Angew. Chem. Int. Ed. Engl.* 30 (1991) 1312–1314.
- [16] H. William, A. Valdesir, R. Gonzalez, *Electrochim. Acta* 47 (2002) 3715–3722.
- [17] J. Lee, J. Seo, K. Han, H. Kim, *J. Power Sources* 163 (2006) 349–356.
- [18] C. Coutanceau, A.F. Rakotonrainibe, A. Lima, E. Garnier, S. Pronier, J.-M. Leger, C. Lamy, *J. Appl. Electrochem.* 34 (2004) 61–66.
- [19] Z.D. Wei, S.H. Chan, *J. Electroanal. Chem.* 569 (2004) 23–33.
- [20] K.H. Choi, H.S. Kim, T.H. Lee, *J. Power Sources* 75 (1998) 230–235.
- [21] D. Lendolt, A. Marlot, *Surf. Technol.* 169–170 (2003) 8–13.
- [22] O. Dossenbach, in: J.-C.L. Puippe, F. Leaman (Eds.), *Theory and Practice of Pulse Plating*, AESF Soc., Orlando, FL, 1986, p. 73.
- [23] M. Mastragostino, A. Missiroli, F. Soavi, *J. Electrochem. Soc.* 8 (2) (2005) A110–A114.
- [24] G. Wu, L. Li, B.Q. Xu, *Electrochim. Acta* 50 (2004) 1–10.
- [25] M.C. Tsai, T.K. Yeh, C.H. Tsai, *Mater. Chem. Phys.* 109 (2008) 422–428.
- [26] X. Zhao, G. Sun, L. Jiang, W. Chen, S. Tang, B. Zhou, Q. Xin, *Electrochim. Solid-State Lett.* 8 (3) (2005) A149–A151.
- [27] S.D. Thompson, L.R. Jordan, M. Forsyth, *Electrochim. Acta* 46 (2001) 1657–1663.
- [28] A.J. Dickinson, L.P.L. Carrette, J.A. Collins, K.A. Friedrich, U. Stimming, *J. Appl. Electrochem.* 34 (2004) 975–984.